

# Graded Mesh in Optimal Control of Subdiffusive Models and its Significance in Neumann-Neumann Waveform Relaxation Algorithm

Bankim C. Mandal<sup>[0009-0009-0134-0422]</sup>,  
Soura Sana<sup>[0000-0003-1892-9486]</sup>

## 1 Introduction

Fractional partial differential equations (PDEs) serve as robust modelling instruments for intricate systems, especially those in which the present state is contingent upon the whole of prior states in a defined manner [14, 15, 21]. Since all previous states are involved in the computation, the computational complexity increases significantly. To tackle this difficulty, parallel computing approaches such as domain decomposition (DD) methods have been established, including Additive Schwarz, Multiplicative Schwarz, and Restrictive Additive Schwarz methods [19, 9, 4]. To further mitigate increased execution time and communication costs associated with large data transfers among processors, waveform relaxation methods were subsequently developed [7] and incorporated into DD frameworks, yielding Schwarz, Neumann-Neumann, Dirichlet-Neumann, and Optimized Schwarz Waveform Relaxation methods [6, 10, 5, 16, 17, 11].

The well-posedness of optimal control problems for diffusive and sub-diffusive systems have been analyzed through coupled system formulations comprising the state system and its adjoint counterpart [8, 12, 13]. Domain decomposition methods have proven effective for PDE-constrained optimization problems [2, 1]. In this work, we apply the NNWR algorithm to solve these coupled systems.

This study is motivated by the work [3] of Ciaramella, Halpern, and Mechelli, where they addressed distributed optimal control problems with time-periodic reaction-diffusion PDEs as constraints using the Optimized Schwarz Waveform Relaxation (OSWR) algorithm. We use semi-discrete analysis to show the convergence of NNWR algorithm for distributed optimal control problems for sub-diffusive PDE.

Let  $[0, T]$  be the time domain with  $T > 0$ , and let  $\Omega$  be an open bounded subset of  $\mathbb{R}^d$  with a boundary  $\partial\Omega$ . The quadratic cost functional is taken into consideration:

---

Bankim C. Mandal · Soura Sana  
School of Basic Sciences, Indian Institute of Technology Bhubaneswar, India, e-mail:  
bmandal@iitbbs.ac.in, ss87@iitbbs.ac.in

$$I(y, u) := \frac{1}{2} \|y - y_{tar}\|_{L^2((0,T) \times \Omega)}^2 + \frac{\sigma}{2} \|u\|_{L^2((0,T) \times \Omega)}^2, \quad (1)$$

where  $u(\mathbf{x}, t)$  be the control variable and  $y_{tar}(\mathbf{x}, t)$  be the target state.  $\sigma$  be the regularization parameter. Finding the ideal control  $u(\mathbf{x}, t)$  that minimizes the cost functional  $I(y, u)$ , while driving the state variable  $y(\mathbf{x}, t)$  toward the target state  $y_{tar}(\mathbf{x}, t)$  is our goal.

The fractional diffusion equation of order  $0 < \beta < 1$  governing the state variable  $y(\mathbf{x}, t)$ , is as follows:

$$\begin{cases} D_{RL}^\beta y(t, \mathbf{x}) = \nabla \cdot (\kappa(t, \mathbf{x}) \nabla y(t, \mathbf{x})) + f(t, \mathbf{x}) + u(t, \mathbf{x}), & \text{in } (0, T) \times \Omega, \\ y(t, \mathbf{x}) = g(t, \mathbf{x}), & \text{on } (0, T) \times \partial\Omega, \\ J_{RL}^{1-\beta} y(0^+, \mathbf{x}) = y_0(\mathbf{x}), & \text{in } \Omega. \end{cases} \quad (2)$$

Here,  $\kappa(t, \mathbf{x}) > 0$  be the diffusion coefficient, and the left-sided Riemann-Liouville fractional derivative in time is defined below:

$$D_{RL}^\beta f(t) := \frac{1}{\Gamma(1-\beta)} \frac{d}{dt} \int_0^t (t-s)^\beta f(s) ds.$$

Additionally, the Riemann-Liouville fractional integral of order  $\beta > 0$  is denoted by  $J_{RL}^\beta$  and defined as the following:

$$J_{RL}^\beta f(t) := \frac{1}{\Gamma(\beta)} \int_0^t (t-s)^{\beta-1} f(s) ds.$$

For  $f, u \in L^2((0, T) \times \Omega)$  the solution to (2) is unique  $y \in L^2((0, T); H^2(\Omega) \cap H_0^1(\Omega))$  for homogeneous Dirichlet boundary condition, for more details see [13]. Also, for the convex objective functional  $I$  a unique infimum is guaranteed. Given (1) and its solution  $y \in L^2((0, T) \times \Omega)$ , we obtain the adjoint variable  $q \in L^2((0, T) \times \Omega)$  using the Euler-Lagrange optimality conditions. Thus the optimality system [12] satisfied by  $(u, y, q)$  is:

$$\begin{cases} D_{RL}^\beta y(t, \mathbf{x}) = \nabla \cdot (\kappa(t, \mathbf{x}) \nabla y(t, \mathbf{x})) + f(t, \mathbf{x}) + u(t, \mathbf{x}), & \text{in } (0, T) \times \Omega, \\ y(t, \mathbf{x}) = g(t, \mathbf{x}), & \text{on } (0, T) \times \partial\Omega, \\ J_{RL}^{1-\beta} y(0^+, \mathbf{x}) = y_0(\mathbf{x}), & \text{in } \Omega. \end{cases} \quad (3)$$

$$\begin{cases} {}_T D_t^\beta p(t, \mathbf{x}) = \nabla \cdot (\kappa(t, \mathbf{x}) \nabla q(t, \mathbf{x})) + y(t, \mathbf{x}) - y_{tar}(t, \mathbf{x}), & \text{in } (0, T) \times \Omega, \\ q(t, \mathbf{x}) = 0, & \text{on } (0, T) \times \partial\Omega, \\ q(T, \mathbf{x}) = 0, & \text{in } \Omega. \end{cases} \quad (4)$$

with the condition  $\sigma u = -q$ . Here,  ${}_T D_t^\beta$  be the right-sided Caputo fractional derivative of order  $0 < \beta < 1$ ,

$${}_T D_t^\beta f(t) := -\frac{1}{\Gamma(1-\beta)} \int_t^T (s-t)^{-\beta} f^{(1)}(s) ds.$$

## 2 The Neumann-Neumann Waveform Relaxation algorithm

We are studying the NNWR algorithm for (3)- (4) for a multi-subdomain scenario. This algorithm contains two parts namely, Dirichlet part and Neumann part. First we solve the Dirichlet part using the initial guesses as Dirichlet boundary conditions on the artificial boundaries, then we calculate the Neumann boundary conditions using the solutions from the Dirichlet part on the artificial boundaries and solve the Neumann part, then we update the initial guesses for the Dirichlet part using the solutions from the Neumann part.

We split the spatial domain  $\Omega$  into multiple non-overlapping subdomains  $\Omega_i$ , where  $1 \leq i \leq M$ , and has no cross point. The intersection of  $\partial\Omega_i$  and  $\partial\Omega_j$  for  $j = i - 1, i + 1$  is expressed as  $\partial\Omega_{i,j}$ . Unit outward normals  $\mathbf{n}_{i,i-1}$  and  $\mathbf{n}_{i,i+1}$  are used on the interfaces  $\partial\Omega_{i,i-1}$  and  $\partial\Omega_{i,i+1}$  on each subdomain  $\Omega_i$ . Given initial guesses  $\xi_{i,j}^{(0)}(\mathbf{x}, t)$  for the state equation and  $\zeta_{i,j}^{(0)}(\mathbf{x}, t)$  for the adjoint equation along the interfaces  $(0, T) \times \partial\Omega_{i,j}$ , the NNWR algorithm can be expressed as follows:

**Dirichlet part:**

**Neumann part:**

$$\begin{cases} D_{RL}^\beta y_i^{(k)} = \nabla \cdot (\kappa_i \nabla y_i^{(k)}) + f - \frac{q_i^{(k)}}{\sigma}, \\ J_{RL}^{1-\beta} y_i^{(k)}(0, \mathbf{x}) = y_0(\mathbf{x}), \\ y_i^{(k)} = g, \\ y_i^{(k)} = \xi_{i,j}^{(k-1)}, \end{cases} \begin{cases} D_{RL}^\beta \psi_i^{(k)} = \nabla \cdot (\kappa_i \nabla \psi_i^{(k)}) - \frac{\chi_i^{(k)}}{\sigma}, \\ J_{RL}^{1-\beta} \psi_i^{(k)}(0, \mathbf{x}) = 0, \\ \psi_i^{(k)} = 0, \\ \kappa_i \partial_{\mathbf{n}_{i,j}} \psi_i^{(k)} = \kappa_i \partial_{\mathbf{n}_{i,j}} y_i^{(k)} + \kappa_j \partial_{\mathbf{n}_{j,i}} y_j^{(k)}. \end{cases} \quad (5)$$

$$\begin{cases} {}_T D_t^\beta q_i^{(k)} = \nabla \cdot (\kappa_i \nabla q_i^{(k)}) + y_i^{(k)} - y_{tar} |_i, \\ q_i^{(k)}(T, \mathbf{x}) = 0, \\ q_i^{(k)} = 0, \\ q_i^{(k)} = \zeta_{i,j}^{(k-1)}, \end{cases} \begin{cases} {}_T D_t^\beta \chi_i^{(k)} = \nabla \cdot (\kappa_i \nabla \chi_i^{(k)}) + \psi_i^{(k)}, \\ \chi_i^{(k)}(T, \mathbf{x}) = 0, \\ \chi_i^{(k)} = 0, \\ \kappa_i \partial_{\mathbf{n}_{i,j}} \chi_i^{(k)} = \kappa_i \partial_{\mathbf{n}_{i,j}} q_i^{(k)} + \kappa_j \partial_{\mathbf{n}_{j,i}} q_j^{(k)}. \end{cases} \quad (6)$$

The following formulae are then used to update the interface values:

$$\xi_{i,j}^{(k)}(t, \mathbf{x}) = \xi_{i,j}^{(k-1)}(t, \mathbf{x}) - \theta_{i,j} \left( \psi_i^{(k)} \Big|_{(0,T) \times \partial\Omega_{i,j}} + \psi_j^{(k)} \Big|_{(0,T) \times \partial\Omega_{i,j}} \right), \quad (7)$$

$$\zeta_{i,j}^{(k)}(t, \mathbf{x}) = \zeta_{i,j}^{(k-1)}(t, \mathbf{x}) - \phi_{i,j} \left( \chi_i^{(k)} \Big|_{(0,T) \times \partial\Omega_{i,j}} + \chi_j^{(k)} \Big|_{(0,T) \times \partial\Omega_{i,j}} \right), \quad (8)$$

Our goal is to examine the convergence of the error equations obtained from (5)-(8).

## 3 Mesh Grading and Convergence Result

We know that utilizing graded mesh (one-sided) [20] over time yields a higher order of accuracy in subdiffusion, denoted as  $O(m^{-(2-\beta)})$ , compared to a uniform mesh (equi-spaced), which offers an accuracy of  $O(m^{-\beta})$ , where  $\beta$  represents the fractional order and  $m$  denotes the number of nodes.

In control problems, solving both the state and adjoint equations necessitates extending the one-sided graded mesh approach to a both-sided grading. Let's consider



### 4 Numerical Experiments

We conduct numerical experiments for the equations (3)–(4), considering homogeneous initial conditions and without any forcing term in the state equation. The computational domain is chosen as  $[-4, 4] \times [0, 1]$ . The diffusion coefficient is set to  $\kappa = 1$ , and the regularization parameter as  $\sigma = 10^{-6}$ . The boundary  $\partial\Omega$  is subject to homogeneous Dirichlet boundary conditions. The following is the target condition:

$$y_{tar}(x, t) = (1 + \tanh(t)) \sin(2\pi x) \left( \exp(-5(x - 0.3)^2) + \exp(-5(x + 0.3)^2) \right). \tag{10}$$

We employ the L1 scheme for temporal integration and a central finite difference scheme for spatial discretisation for the sub-diffusion problem. The simulation continues until the Dirichlet trace’s relative error drops below the  $10^{-10}$  tolerance level. We discretise the time period using 100 temporal nodes and set the spatial step size to  $\Delta x = 0.05$ . As seen in Fig. 1, we calculate the solution, control, and target profiles using a fractional order of  $\alpha = 0.6$ . Because of the abrupt change brought about by the homogeneous initial condition, the figure shows that the control component has a greater effect close to the initial time  $t = 0$ .

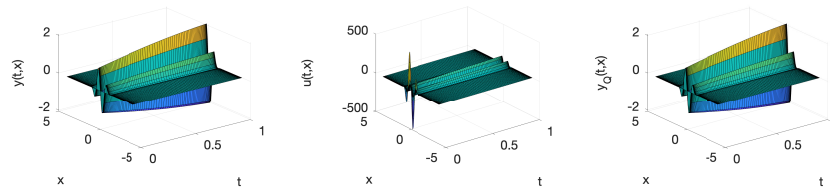


Fig. 1: Monodomain: solution state (left), control state (middle), and target state (right).

#### 4.1 Eigenvalue Comparison

For varying numbers of temporal discretization nodes and three distinct discretization methods, we investigate in Fig. 2 the change in the minimal real part of the square root of the eigenvalues of  $\mathbb{D}$ , represented by  $\min \Re \left( \sqrt{\lambda(\mathbb{D})} \right)$ . For both the uniform and one-sided graded meshes, we observe that  $\min \Re \left( \sqrt{\lambda(\mathbb{D})} \right)$  increases gradually as the number of temporal nodes increases more noticeably for lower fractional orders, and more moderately for higher ones. In contrast, the both-sided graded mesh shows a different behavior: after an initial rapid increase, the value plateaus and remains nearly constant. The convergence rate, which will be further examined in the next plots, is directly impacted by this behavior.

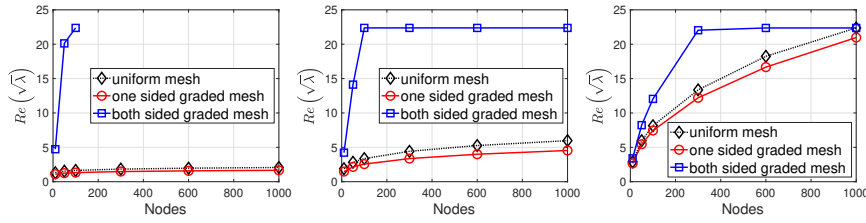


Fig. 2: For time fractional order, the minimum value of the real component of the square root of the time matrix’s eigenvalues in the time domain  $(0, 1)$ , left:  $\beta = 0.2$ , middle:  $\beta = 0.5$  and right:  $\beta = 0.9$ .

### 4.2 NNWR Algorithm

We divide the physical region  $\Omega = (-4, 4)$  into many non-overlapping subdomains for the NNWR experiments. These trials are conducted using the same target profile as specified in (10).

Before proceeding, we numerically justify the choice of relaxation parameters for the NNWR algorithm. In order to achieve this, we take into account three subdomains with different lengths:  $a_1 = 2, a_2 = 4$ , and  $a_3 = 2$ , each assigned a different diffusion coefficient:  $\kappa_1 = 0.36, \kappa_2 = 0.81$ , and  $\kappa_3 = 0.36$ , respectively.

Through numerical experimentation, we observe that selecting relaxation parameters as  $\theta_i = \phi_i = 1/(2 + \sqrt{\kappa_i/\kappa_{i+1}} + \sqrt{\kappa_{i+1}/\kappa_i})$  yields improved convergence behavior. Specifically, Fig. 3 shows that the values  $\theta_1 = 0.24$  and  $\theta_2 = 0.24$  (indicated by red stars) achieve the most favorable convergence after 10 iterations, outperforming all other values of  $\theta_1$  and  $\theta_2$  in  $(0, 0.5)$ . Notably, these relaxation parameters are largely independent of the fractional order  $\beta$ . As a result, we adopt the formula consistently in all subsequent NNWR experiments.

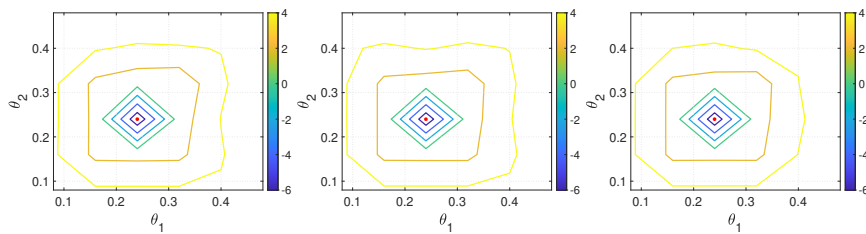


Fig. 3: NNWR: For three subdomain cases with subdomain length,  $a_1 = 1, a_2 = 4, a_3 = 3$ , and diffusion coefficients  $\kappa_1 = 0.36, \kappa_2 = 0.81, \kappa_3 = 0.36$ , the numerical convergence rate in log scale for various  $\theta$  after 10 iterations with  $T = 1$ ; left:  $\beta = 0.2$ , middle:  $\beta = 0.6$ , and right:  $\beta = 0.99$  for both sided graded mesh.

Using the time frame of  $T = 5$ , we examine the convergence rates of the NNWR method for the state solution across various values of the fractional order  $\beta$  in Fig. 4

and Fig. 5. The domain  $\Omega = (-4, 4)$  is divided into five subdomains in both the equal and unequal subdomain cases. In the case of equal subdomains, the diffusion coefficient  $\kappa_i = 1$  is constant. We define the subdomains in the case of unequal subdomains as follows:  $\Omega_1 = (-4, -3)$ ,  $\kappa_1 = 0.25$ ;  $\Omega_2 = (-3, -1.5)$ ,  $\kappa_2 = 1$ ;  $\Omega_3 = (-1.5, 1)$ ,  $\kappa_3 = 0.25$ ;  $\Omega_4 = (1, 2.5)$ ,  $\kappa_4 = 4$  and  $\Omega_5 = (2.5, 4)$ ,  $\kappa_5 = 1$ . The numerical findings show that, when uniform and one-sided graded meshes are used, the fractional order  $\beta$  has a considerable impact on the NNWR algorithm's convergence rate. However, for the both-sided graded mesh, the convergence rate appears less sensitive to changes in  $\beta$ . This observation aligns with the behavior illustrated in Fig. 2, where variations in  $\min \Re(\sqrt{\lambda(\mathbb{D})})$  are shown for different types of mesh grading.

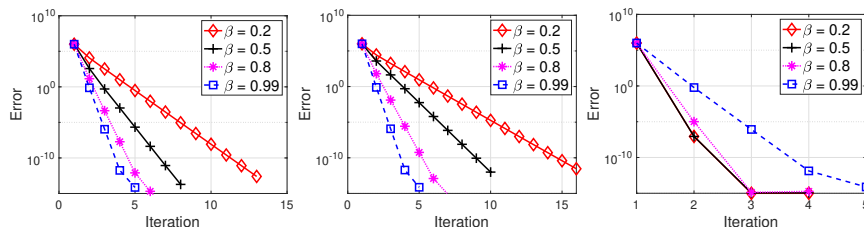


Fig. 4: NNWR: Numerical convergence rate for various fractional orders  $\beta$  for  $\theta = 0.25$  with fixed  $T = 5$ ; Uniform mesh in time on the left, one-sided graded mesh in time in the middle, and both-sided graded mesh in time on the right.

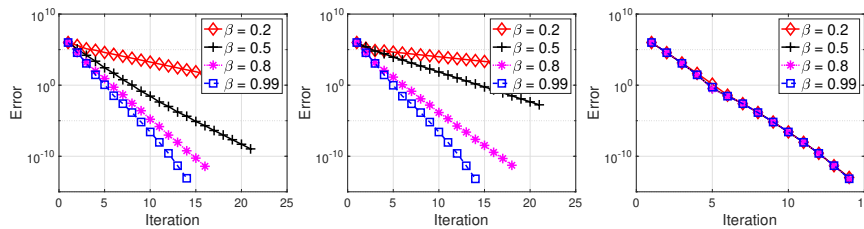


Fig. 5: NNWR: The numerical convergence rate for various fractional orders  $\beta$  with fixed  $T = 5$ ; with uneven subdomain size and  $\kappa$ , where, Left: uniform mesh in time; middle: one-sided graded mesh in time; right: both-sided graded mesh in time;  $\Omega_1 = (-4, -3)$ ,  $\kappa_1 = 0.25$ ;  $\Omega_2 = (-3, -1.5)$ ,  $\kappa_2 = 1$ ;  $\Omega_3 = (-1.5, 1)$ ,  $\kappa_3 = 0.25$ ;  $\Omega_4 = (1, 2.5)$ ,  $\kappa_4 = 4$ ;  $\Omega_5 = (2.5, 4)$ ,  $\kappa_5 = 1$ .

## References

1. Benamou, J.D.: A domain decomposition method for control problems. In: Proc. DD9, pp. 266–273 (1998)
2. Bensoussan, A., Glowinski, R., Lions, J.L.: Decomposition method applied to the optimal control of distributed systems. In: IFIP Tech. Conf. Optim. Tech., pp. 141–151 (1973)
3. Ciaramella, G., Halpern, L., Mechelli, L.: Convergence analysis and optimization of a Robin Schwarz waveform relaxation method for time-periodic parabolic optimal control problems. *J. Comput. Phys.* **496**, 112572 (2024)
4. Dryja, M., Widlund, O.B.: Some domain decomposition algorithms for elliptic problems. In: Iterative Methods for Large Linear Systems, pp. 273–291. Elsevier (1990)
5. Gander, M.J., Kwok, F., Mandal, B.C.: Dirichlet–Neumann and Neumann–Neumann waveform relaxation algorithms for parabolic problems. *ETNA* **45**, 424–456 (2016)
6. Gander, M.J., Stuart, A.M.: Space-time continuous analysis of waveform relaxation for the heat equation. *SIAM J. Sci. Comput.* **19**(6), 2014–2031 (1998)
7. Lelarasmee, E.: The waveform relaxation method for time-domain analysis of large-scale integrated circuits: theory and applications. Electronics Research Laboratory, College of Engineering (1982)
8. Lions, J.L.: Some aspects of the optimal control of distributed parameter systems. *SIAM* (1972)
9. Lions, P.L.: On the Schwarz alternating method. III: A variant for nonoverlapping subdomains. In: Third Int. Symp. Domain Decomposition Methods Partial Differ. Equ., vol. 6, pp. 202–223. SIAM (1990)
10. Mandal, B.C.: Neumann–Neumann waveform relaxation algorithm in multiple subdomains for hyperbolic problems in 1D and 2D. *Numer. Methods Partial Differ. Equ.* **33**(2), 514–530 (2017)
11. Mandal, B.C., Sana, S.: Substructuring waveform relaxation methods with time-dependent relaxation parameter. In: Proc. Sixth Int. Conf. Math. Comput. (ICMC 2020), pp. 429–440. Springer (2021)
12. Mophou, G.M.: Optimal control of fractional diffusion equation. *Comput. Math. Appl.* **61**(1), 68–78 (2011)
13. Mophou, G.M., N’Guérékata, G.M.: Optimal control of a fractional diffusion equation with state constraints. *Comput. Math. Appl.* **62**(3), 1413–1426 (2011)
14. Povstenko, Y., Kyrlylych, T.: Fractional thermoelasticity problem for an infinite solid with a penny-shaped crack under prescribed heat flux across its surfaces. *Philos. Trans. R. Soc. A* **378**(2172), 20190289 (2020)
15. Qin, S., Liu, F., Turner, I., Vegh, V., Yu, Q., Yang, Q.: Multi-term time-fractional Bloch equations and application in magnetic resonance imaging. *J. Comput. Appl. Math.* **319**, 308–319 (2017)
16. Sana, S., Mandal, B.C.: Dirichlet–Neumann and Neumann–Neumann waveform relaxation algorithms for heterogeneous sub-diffusion and diffusion-wave equations. *Comput. Math. Appl.* **150**, 102–124 (2023)
17. Sana, S., Mandal, B.C.: Convergence analysis of the Dirichlet–Neumann waveform relaxation algorithm for time-fractional sub-diffusion and diffusion-wave equations in heterogeneous media. *Adv. Comput. Math.* **50**(4), 91 (2024)
18. Sana, S., Mandal, B.C.: Optimal control of a sub-diffusion model using Dirichlet–Neumann and Neumann–Neumann waveform relaxation algorithms (2025)
19. Schwarz, H.A.: Über einen Grenzübergang durch alternierendes Verfahren. *Zürcher u. Furrer* (1870)
20. Stynes, M., O’Riordan, E., Gracia, J.L.: Error analysis of a finite difference method on graded meshes for a time-fractional diffusion equation. *SIAM J. Numer. Anal.* **55**(2), 1057–1079 (2017)
21. Sun, H., Zhang, Y., Baleanu, D., Chen, W., Chen, Y.: A new collection of real-world applications of fractional calculus in science and engineering. *Commun. Nonlinear Sci. Numer. Simul.* **64**, 213–231 (2018)